ELSEVIER

Contents lists available at ScienceDirect

Organic Geochemistry

journal homepage: www.elsevier.com/locate/orggeochem





Heterotrophic origin and diverse sources of branched glycerol monoalkyl glycerol tetraethers (brGMGTs) in peats and lignites

Felix J. Elling a,b,1,*, Laura Kattein a,1,2, B. David A. Naafs c, Vittoria Lauretano c, Ann Pearson a

- ^a Department of Earth and Planetary Sciences, Harvard University, Cambridge, MA 02138, USA
- ^b Leibniz-Laboratory for Radiometric Dating and Isotope Research, Christian-Albrecht University of Kiel, 24118 Kiel, Germany
- ^c Organic Geochemistry Unit, School of Chemistry and Cabot Institute, University of Bristol, UK

ARTICLE INFO

Associate Editor-Rienk Smittenberg

Keywords:
BrGMGTs
H-shaped brGDGTs
Compound-specific carbon stable isotope
analysis
Spooling-Wire Microcombustion IRMS

ABSTRACT

The branched glycerol monoalkyl glycerol tetraether lipids of bacteria (brGMGTs, sometimes referred to as HbrGDGTs) are found in marine, lacustrine, and terrestrial mesophilic environments. The abundance of brGMGTs relative to their dialkyl analogues (brGDGTs) has been proposed as a proxy for past continental air and lake water temperature. However, the source(s) of brGMGTs remain unknown. brGDGT production has been described in multiple cultivated Acidobacteria, but so far no brGMGT producer has been identified. We hypothesize that the stable carbon isotopic composition (δ^{13} C) of brGMGTs, as a tracer of carbon source and metabolic pathway, could be used to elucidate the source(s) of brGMGTs relative to brGDGTs. However, the large monoalkyl moiety of these compounds impedes carbon isotopic analysis using conventional techniques based on gas chromatography. Here, we used Spooling-Wire Microcombustion to analyse the stable carbon isotopic composition of brGMGTs and brGDGTs found in peats and lignites. We show that the δ^{13} C of brGMGTs is within ~ 2 % similar to that of brGDGTs from the same samples, as well as the δ^{13} C of the total organic carbon. This suggests that the source organisms use heterotrophic metabolisms. However, offsets in the δ^{13} C of brGDGTs and brGMGTs in some samples suggest that not all brGDGT producers also produce brGMGTs. Further, in modern peats we observe downcore increases in brGMGT relative abundance and decreases in the carbon isotopic offsets with brGDGTs, which indicates that brGMGT producers occur throughout the oxic-anoxic continuum and may metabolize different organic carbon pools. Based on this indirect evidence for diverse brGMGT sources, we suggest that in addition to homeostatic responses to temperature, brGMGT relative abundances may be influenced by changes in bacterial community composition in response to additional environmental and biogeochemical parameters.

1. Introduction

Glycerol dialkyl glycerol tetraethers (GDGTs) and their derivatives are ubiquitous in modern soils and the ocean as well as the geologic record (Schouten et al., 2000, 2013). Due to their source-specificity and diagenetic stability, GDGTs are important biomarkers used in paleoclimate reconstructions (Pearson and Ingalls, 2013; Schouten et al., 2013) and as tracers for distinct groups of archaea and bacteria in the modern environment (Schouten et al., 2013). GDGTs are classified into two major groups, isoprenoid GDGTs (iGDGTs) occurring in archaea and branched GDGTs (brGDGTs) occurring in bacteria (Rosa et al., 1986; Weijers et al., 2006, 2009; Sinninghe Damsté et al., 2014; Halamka

et al., 2021, 2022; Chen et al., 2022). The iGDGTs are composed of two C₄₀ isoprenoid sidechains (biphytanes) terminally ether-bound to two glycerol moieties, thus forming a macrocyclic tetraether lipid (Langworthy, 1977). brGDGTs are structural analogues of iGDGTs with non-isoprenoid methyl-branched alkanes instead of biphytanes and distinct stereochemistry (Sinninghe Damsté et al., 2000; Weijers et al., 2006). Both iGDGTs and brGDGTs may possess a number of structural modifications, the most prominent being a varying number of methylations (Weijers et al., 2006; Liu et al., 2012; Zhu et al., 2014; Knappy et al., 2015) and cyclopentane rings in the sidechains (Rosa et al., 1986; Weijers et al., 2006; Liu et al., 2016). Besides the commonly investigated iGDGTs and brGDGTs, many GDGT derivatives occur in the environment

^{*} Corresponding author at: Leibniz-Laboratory for Radiometric Dating and Isotope Research, Christian-Albrecht University of Kiel, 24118 Kiel, Germany. E-mail address: felling@leibniz.uni-kiel.de (F.J. Elling).

¹ These authors contributed equally.

² Present address: Laura Kattein, Alfred Wegener Institute, Helmholtz Center for Polar and Marine Sciences, 27570 Bremerhaven, Germany.

but lack known source organisms (Liu et al., 2012). Understanding the sources, fates, and parameters influencing the distributions of these 'orphan biomarkers' (Brocks and Pearson, 2005) may lead to new insights into microbial adaptation to environmental stresses and to the discovery of novel paleoenvironmental proxies.

The glycerol monoalkyl glycerol tetraethers (GMGTs) are a structurally distinct class of 'orphan' GDGT derivatives in which the sidechains are covalently linked through a central carbon-carbon bond (Morii et al., 1998), forming an H-shaped C_{80} core structure. GMGTs with an isoprenoid monoalkyl structure were first described in thermophilic archaea (Morii et al., 1998; Sugai et al., 2004; Knappy et al., 2011; Liu et al., 2012), although they are now known also to occur in mesophilic environments (Schouten et al., 2008; Naafs et al., 2018a). Similar to archaeal GMGTs, branched GMGTs (brGMGTs) are abundant in mesophilic environments, including marine sediments (Liu et al., 2012; Bijl et al., 2021; Kirkels et al., 2022), oxygen minimum zones (Xie et al., 2014), lacustrine sediments (Baxter et al., 2019), mineral soils, wetlands, and lignites (fossilized peat; Naafs et al., 2018a; Lü et al., 2019; Tang et al., 2021). The branched monoalkyl structure suggests a bacterial origin of brGMGTs, analogous to brGDGTs. brGMGT abundance is positively correlated with temperature in modern peats and lake sediments, suggesting a physiological role in membrane homeostasis and potential use as a paleotemperature proxy (Liu et al., 2012; Naafs et al., 2018a, 2018b; Baxter et al., 2019; Sluijs et al., 2020; Tang et al., 2021). However, the sources of brGMGTs and their relationships with producers of regular brGDGTs remain unresolved as they have not been observed in cultivated bacteria.

Compound-specific carbon isotopic analysis could help constrain both the origin of brGMGTs in environmental samples and the carbon sources of their producers. However, brGMGTs are not amenable to conventional gas chromatography-isotope ratio mass spectrometry (IRMS) due to the large C_{80} core structure. The stable carbon isotopic compositions of brGMGTs thus have not been analysed before. Here, we report the stable carbon isotopic compositions of brGMGTs in peats and two lignites, obtained using Spooling Wire Microcombustion (SWiM)-IRMS (Sessions et al., 2005; Pearson et al., 2016). Carbon isotope systematics of brGDGTs and brGMGTs reveal distinct, heterotrophic sources for these compounds.

2. Materials and Methods

2.1. Sampling and sample preparation

The modern peat cores used in this study were obtained from two locations (SEB1B: 2.3231° S, 113.9039° E; SEB2B: 2.3312° S, 113.8968° E) in the tropical peatland of Sebangau (Borneo, Indonesia). At the location of SEB2B, a parallel core (SEB2B-O) was taken. The cores represent different depth layers. Cores SEB1B and SEB2B profiles were sampled from 0 to 50 cm depth, whereas only samples from the lower part (40–50 cm) were available for SEB2B-O. Two lignite samples (L1 and L2) of Early Miocene age (18.2 and 17.8 Ma, respectively; Korasidis et al., 2019) were obtained from the Morwell 1A formation (M1A seam) in Latrobe Valley (Australia, 38.2544° S, 146.5769° E).

Both peat and lignite samples were freeze-dried, homogenized by mortar and pestle, and 1–2 g sample splits were extracted in Teflon vessels using a CEM Mars microwave extraction system in three steps: (i) 1:1 dichloromethane:methanol, (ii) 9:1 dichloromethane:methanol, and (iii) 100 % dichloromethane. The microwave program consisted of (i) 30 min ramped heating program to 70 °C, (ii) hold at 70 °C for 20 min, (iii) cool-down for 10 min, after which solvent was decanted and fresh solvent added. The extracts were combined into a total lipid extract (TLE), filtered through glass wool, dried under N_2 and stored at –20 °C. TLE aliquots were separated into five fractions over pre-combusted SiO₂ (Pearson et al., 2016). After component quantification using flow injection analysis (FIA), the fractions containing GDGT core lipids and polar components were combined and subsequently filtered through

0.45 µm syringe filters.

2.2. GDGT analysis, purification and isotopic analysis

Core GDGT distributions were analysed using the chromatographic method of Becker et al. (2013) with the modifications described in Polik et al. (2018). Briefly, TLE aliquots were injected into an Agilent 1290 series ultra-high performance liquid chromatograph coupled to an Agilent 6410 series triple-quadrupole mass spectrometer (operated in scan mode) via an atmospheric pressure chemical ionization ion source operating in positive mode.

Individual core GDGTs were purified for $\delta^{13}C$ analysis using orthogonal HPLC. Before each step of HPLC purification, GDGT concentrations were estimated using FIA. Peak areas were compared to a dilution series of a synthetic standard (C46-GTGT) and purified GDGT-0 and crenarchaeol standards. The estimated concentrations were used to limit the quantity of GDGTs injected to $\leq 10~\mu g$ to prevent column overloading and improve peak separation. Different normal and reversed phase HPLC methods were employed to separate individual compounds followed by a final step of clean-up using reversed phase HPLC, as described in detail below.

For the peat samples, individual core GDGTs were isolated from the combined polar fraction using normal phase HPLC following Pearson et al. (2016). The sample was dissolved in 45 μL of 1 % isopropanol in hexane and injected onto an Agilent ZORBAX NH2 column (4.6 \times 250 mm inner diameter; 5 μm particle size) maintained at 35 °C. Compounds were eluted at a flow rate of 1 mL min $^{-1}$ using 100 % eluent A (1.35 % isopropanol in hexane) for 55 min.

For the two lignite samples, individual GDGTs were isolated from the combined polar fraction using normal phase HPLC following a method modified from Liu et al., (2012). The sample was prepared as described above but injected onto a Hichrom Limited Prevail Cyano column (2.1 imes150 mm inner diameter; 3 µm particle size) maintained at 35 °C. Compounds were eluted at a flow rate of 1 mL min⁻¹ using the following program: 100 % eluent A (1.2 % isopropanol in hexane) for 5 min, a linear gradient to 10 % eluent B (10 % isopropanol in hexane) in 30 min, a linear gradient to 100 % B in 10 min, 100 % B for 10 min, followed by re-equilibration at 100 % A for 15 min. brGDGTs and iGMGTs were collected in a combined fraction due to co-elution. These two compound groups were isolated from the mixed fraction using reversed phase HPLC on an Agilent 1290 Infinity Series Liquid Chromatograph, yielding one brGDGT and one iGMGT fraction. Separation was achieved on an ACE3 C_{18} column (2.1 imes 150 mm inner diameter, 3 μ m particle size) using a gradient from methanol (eluent A) to isopropanol (eluent B) as described previously (Zhu et al., 2013), but omitting formic acid and ammonium hydroxide from the eluents. Individual compounds were separated from the brGDGTs fraction by normal phase HPLC on an Agilent 1100 Series Liquid Chromatograph/Mass Selective Detector using an Agilent ZOR-BAX NH2 column as described above.

The individual brGDGT/brGMGT fractions were then purified through reversed phase HPLC on an Agilent ZORBAX Eclipse XDB-C8 column as described by Pearson et al. (2016). Two one-minute fractions were collected for each sample. F1 covered the minute before the GDGTs/GMGTs eluted and was used to measure the background size and $\delta^{13}\text{C}$ value. F2 contained the purified GDGTs/GMGTs.

The purified GDGTs/GMGTs were dried under nitrogen and dissolved in ethyl acetate immediately before SWiM-IRMS analysis (Sessions et al., 2005; Pearson et al., 2016). For each sample, three measurements were conducted on F1 (background) and six on F2 (GDGTs/GMGTs). Data were corrected against a CO $_2$ reference gas and a crenarchaeol standard of known isotopic composition. A dilution series of C $_{46}$ -GTGT was used for quantification as well as peak size and offset corrections (as described in detail in Pearson et al., 2016). To detect the influence of background levels on $\delta^{13}C_{GDGT}$ values, the ratio of F2 and F1 peak areas was calculated for each sample (F2/F1). A cut-off for acceptable $\delta^{13}C_{GDGT}$ values was established as F2/F1 \geq 2. After isotopic

analysis, FIA was performed on the remaining F2 to determine purity calculated as the relative proportion of response-corrected analyte abundance to total ion current. The brGDGT-I δ^{13} C data from SEB2B were previously published in Blewett et al. (2022).

2.3. Elemental analysis

Content and stable carbon isotopic composition of total organic carbon (TOC) were determined on vapor-acidified samples in silver capsules (concentrated HCl, 60 °C, 48 h; wrapped in additional tin capsule before analysis) using an elemental analyser-IRMS (Thermo Flash EA Isolink CN coupled to a Delta V Plus IRMS). Using the same instrument, stable carbon isotopic compositions of TLEs were analysed from 5 μL aliquots (dissolved in 5:1 dichloromethane:methanol) adsorbed onto glass fibre filters (GF-75, Advantec, Japan), with the solvent evaporated at 42 °C for 2 h before wrapping in a tin capsule. Carbon isotopic compositions were blank-corrected, peak-size-corrected, and offset-corrected using laboratory and authentic reference standards. All results are reported in delta notation relative to VPDB.

3. Results

3.1. brGDGT and brGMGT abundance

The distributions of branched tetraether lipids in all samples are dominated by the acyclic tetramethylated brGDGT-Ia (Supplementary Data Table S1), with minor amounts of penta- (brGDGT-II) and hexamethylated (brGDGT-III) homologues as well as low amounts of cyclized derivatives and isomers. For the brGMGTs named H-1020, H-1034, and H-1048 in other publications (Naafs et al., 2018a), we adopted the nomenclature brGMGT-I, -II, and -III, respectively, in analogy to the naming scheme for brGDGTs. Although their exact

structures have not been determined, it is likely that brGMGT-I, -II, and -III represent tetramethylated, pentamethylated, and hexamethylated brGMGTs, respectively, with one of the central methyl groups participating in the bridge that creates the monoalkyl structure. brGMGT-I is the dominant brGMGT in all samples (97 % of brGMGTs in peats, 82 % in lignites). In the peat cores, the %brGMGTs (brGMGTs/(brGMGTs + brGDGTs)) increases with depth from ~ 2 % to ~ 20 %. In the two lignite samples, brGMGTs make up 10 % and 43 % of the tetraether lipids. Concentrations (expressed as peak area/g dry sediment) of individual and bulk brGMGTs and brGDGTs increase with depth (Fig. S2, Supplementary Data Table S1).

3.2. Carbon isotopic composition

Stable carbon isotopic compositions (δ^{13} C vs VPDB) were successfully measured for all bulk samples (TOC and TLE) and for the dominant individual compounds (brGDGT-I and brGMGT-I) in most samples. For some samples, concentrations of brGDGT-I or brGMGT-I were below detection or data quality was not within the normally acceptable range previously determined for iGDGTs (F2/F1 ratio > 2; Polik et al., 2018; Elling et al., 2019; Blewett et al., 2022). However, for most samples with F2/F1 < 2, purity was > 90 %, with no apparent relationship between δ^{13} C and F2/F1 or peak size in IRMS (Fig. S1), suggesting no influence of the background or analyte concentration on carbon isotopic compositions. Therefore, these data were retained for subsequent data analysis.

Generally, the $\delta^{13}\text{C}$ values of brGDGT-I and brGMGT-I are broadly similar to each other and to TOC and TLE (Figs. 1 & 2). In the modern peat samples (cores SEB1B, SEB2B and SEB2B-O) the bulk samples and individual compounds range between –31 ‰ and –34 ‰. The two lignite samples are distinct from the peats, with $\delta^{13}\text{C}$ values ranging from –27 ‰ to –28 ‰ in the bulk samples and –28 ‰ to –31 ‰ for the individual compounds. The $\delta^{13}\text{C}$ values of TLE are mostly lower than TOC, by up to

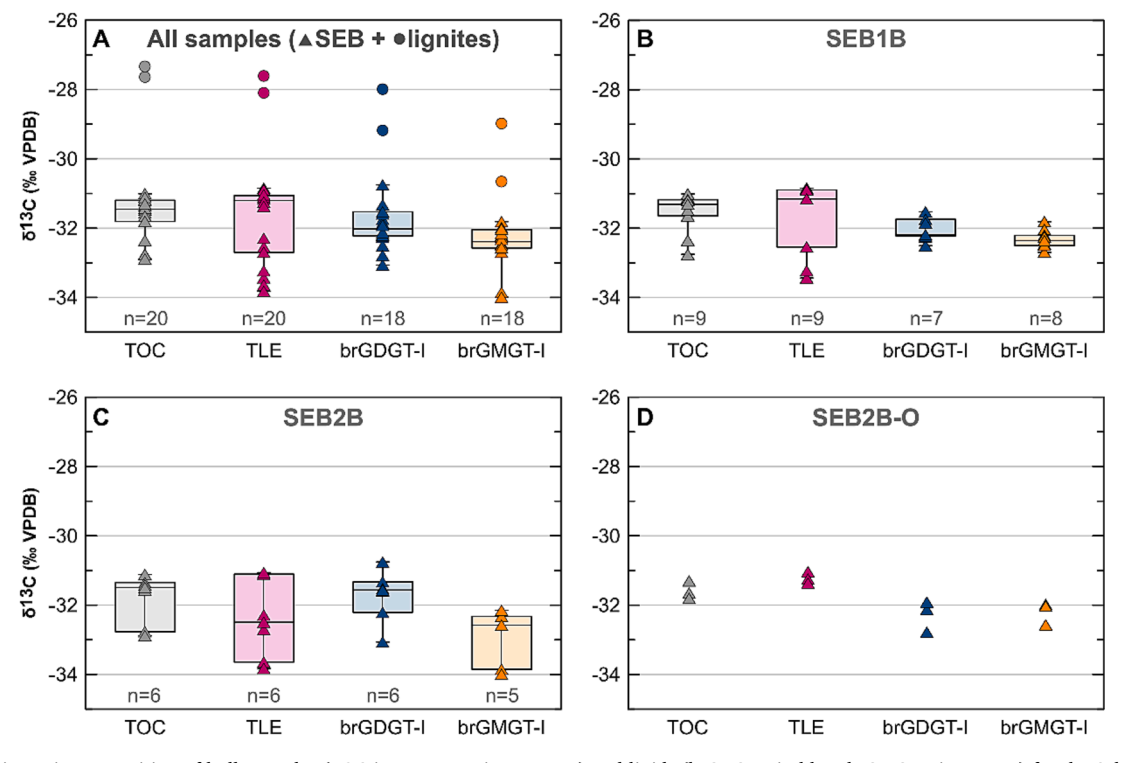


Fig. 1. Carbon isotopic composition of bulk samples (TOC in grey; TLE in magenta) and lipids (brGDGT-I in blue; brGMGT-I in orange) for the Sebangau peatland (SEB, triangles) and the Miocene Morwell 1A lignites (circles). Panel A shows the combined dataset, containing both the SEB samples as well as the two lignite samples that have more enriched δ^{13} C values and are shown as individual data points above the box plots. Panels B, C and D show the data of each of three SEB cores individually. Boxes comprise 50 % of the data points with the upper and lower quartile separated by the median (horizontal line) and whiskers indicate maximum and minimum values. The number n of samples included in the box-whisker-plot is given below each box. If $n \le 3$ (e.g. panel D, SEB2B-O), the data were plotted as individual points only. (For interpretation of the references to colour in this figure legend, the reader is referred to the web version of this article.)

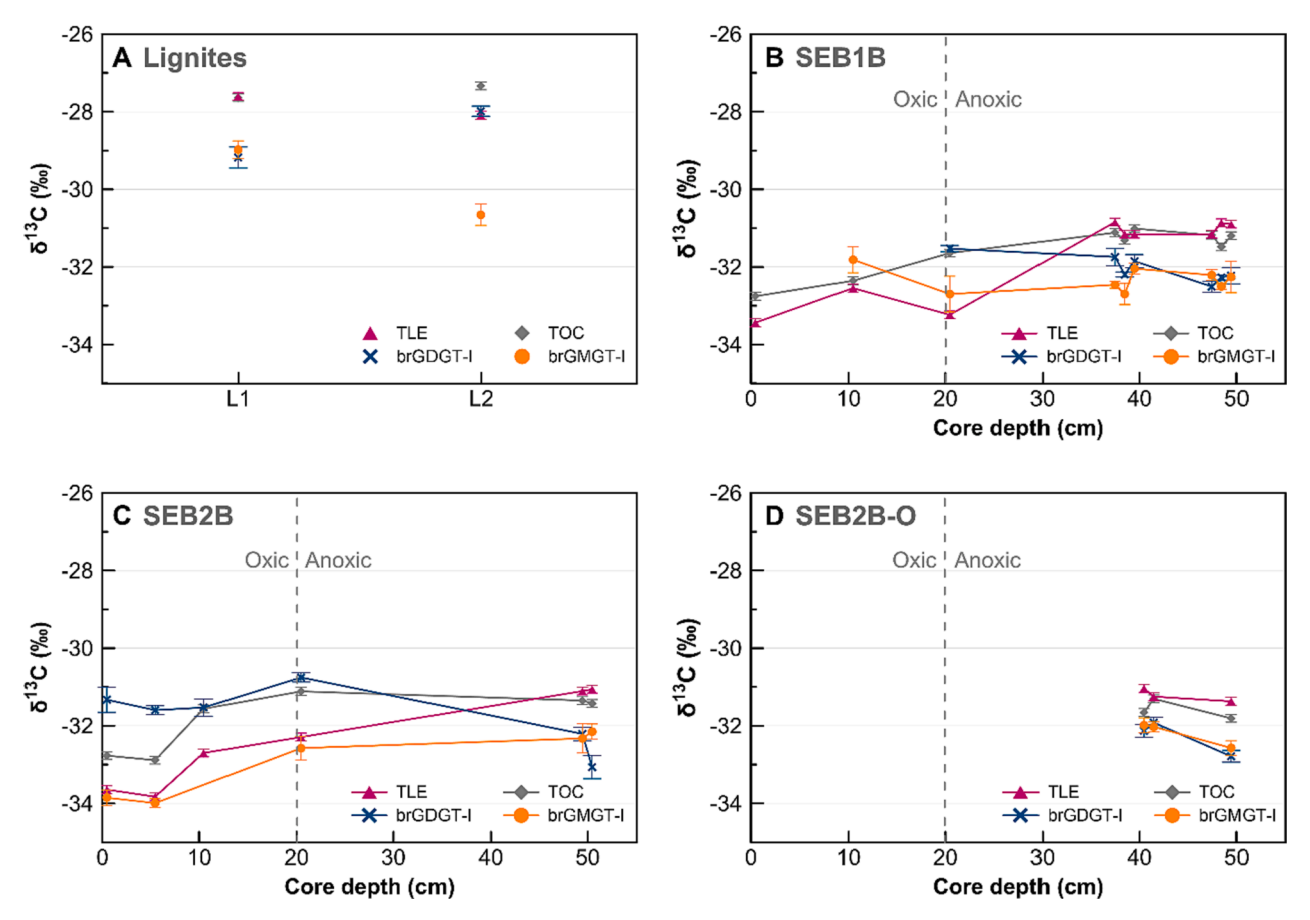


Fig. 2. Downcore profiles of carbon isotopic compositions of total organic carbon (TOC), total lipid extract (TLE), brGDGT-I and brGMGT-I in Miocene Morwell 1A lignites (A) and three peat cores from Sebangau (B-D). The tentative depth of the oxic-anoxic transition is indicated by a stippled vertical line.

2 ‰. The δ^{13} C values of brGMGT-I are mostly lower than the values for TOC, TLE, and brGDGT-I, by up to 2 ‰. The δ^{13} C values of brGDGT-I are mostly lower than the values for TOC and TLE.

The bulk and compound-specific $\delta^{13}C$ values vary with depth at each site (Fig. 2). The $\delta^{13}C$ values of TOC are generally higher than the values for TLE but both increase and converge at greater depth. In SEB1B, $\delta^{13}C$ values of brGDGT-I and brGMGT-I decrease or stay invariant; however, the record is incomplete as $\delta^{13}C$ values could not be determined for the upper part of the core. In SEB2B, $\delta^{13}C$ values of brGDGT-I and brGMGT-I increase with depth, except for the deepest samples. In most samples, the $\delta^{13}C$ value of brGDGT-I is higher than the $\delta^{13}C$ value of brGMGT-I (by \sim 1 % in SEB1B, 2 % in SEB2B), except for the deepest core depths (~deeper than 40 cm) where brGDGT-I and brGMGT-I $\delta^{13}C$ values converge. Due to the limited number of lignite and SEB2B-O samples, trends are only described for SEB1B and SEB2B samples.

4. Discussion

4.1. Microbial degradation of organic matter

The carbon isotopic composition of fresh organic matter in soil is primarily determined by plant isotope fractionation during carbon fixation and biosynthesis (Smith, 1972). Kinetic isotope fractionation and preferential degradation during microbial respiration of organic matter alters $\delta^{13}C_{TOC}$ (Stout et al., 1981). During organic matter respiration, microbes discriminate against ^{13}C , leaving the remaining organic matter ^{13}C -enriched by 1–3 ‰ (Stout et al., 1981; Natelhoffer and Fry, 1988; Balesdent et al., 1993; Novák et al., 1999; Esmeijer-Liu et al., 2012). Although the Suess effect (change of $\delta^{13}C$ of atmospheric CO₂ by input of anthropogenic $^{12}CO_2$) alone can account for downcore ^{13}C -enrichment

of up to 2 % in tropical soils (Wu et al., 2019), it cannot be the sole cause for the downcore ¹³C-enrichment seen in the Sebangau peat cores due to their relatively young age. Even though there is no age model available for our samples, the age can be inferred from two cores taken less than 10 km from our sample locations (Weiss et al., 2002; Wüst et al., 2008). In this context, the bases of the Sebangau peat cores are likely younger than 100 years old. Additionally, the $\delta^{13}C_{TOC}$ profiles in SEB1B and SEB2B show the steepest slope close to the surface (i.e., within the first 10-20 cm), which is indicative of early microbial diagenesis, while the Suess effect should be visible over much broader depths in the core. Nevertheless, since dilution of the atmosphere with ¹²CO₂ is an ongoing process, it likely contributed to lower bulk and lipid δ^{13} C values observed towards the top of the cores. The increase of $\delta^{13}C_{TOC}$ with depth in the Sebangau peat cores (Fig. 2) is thus primarily caused by microbial respiration since deposition, with only minor amplification of this trend attributed to expression of the Suess effect.

Preferential degradation of ^{13}C -depleted organic matter is also reflected in the $\delta^{13}\text{C}$ trend observed in the TLE fraction. In all samples taken within the first 20 cm, $\delta^{13}\text{C}_{TLE}$ values are lower than $\delta^{13}\text{C}_{TOC}$ values, which reflects the primary signature of the biosynthetic pathways of bulk biomass (primarily protein and carbohydrates, relatively ^{13}C -enriched) and lipids (relatively ^{13}C -depleted; Hayes, 2001). Convergence of $\delta^{13}\text{C}_{TLE}$ and $\delta^{13}\text{C}_{TOC}$ at depth may reflect (i) enhanced respiration of lipids, which may result from depletion of other (preferred) carbon substrates at this depth, or (ii) biosynthesis of large amounts of lipids with $\delta^{13}\text{C}$ similar to $\delta^{13}\text{C}_{TOC}$ (e.g., via acetate derived from fermentation of TOC with negligible ^{13}C -fractionation). The depth of enhanced lipid respiration below 20 cm coincides with the mean annual ground water level in the Sebangau peat swamp, which was -23 cm and -39 cm in 2014 and 2015, respectively (Itoh et al., 2017). In peat

swamps, ground water levels control the availability of oxygen needed for aerobic respiration (Clymo, 1984). Together with the $\delta^{13}C_{TOC}$ profile, the $\delta^{13}C_{TLE}$ profile thus suggests that organic matter is intensely aerobically respired in the upper 20 cm and to a lesser degree anaerobically or micro-aerobically degraded below 20 cm depth. This transition zone is reflected in the abundance of brGDGTs and brGMGTs (discussed below; Fig. 2 & S2) with lower concentrations in the oxic zone ($\sim\!0\text{--}20$ cm) and higher concentrations in the anoxic zone ($\sim\!38\text{--}50$ cm; no data between 20 and 38 cm). This is consistent with previous work (Naafs et al., 2019) and suggests that brGDGTs and brGMGTs that are present throughout the core can be sourced from producers using different metabolisms under contrasting availability of oxygen and carbon sources.

4.2. Heterotrophic origin of brGDGTs and brGMGTs

Heterotrophic bacteria have been suggested as source organisms of brGDGTs in various environments, such as peat (Pancost and Sinninghe Damsté, 2003; Weijers et al., 2009; Huguet et al., 2017; Naafs et al., 2017; Blewett et al., 2022), loess type soil (Weijers et al., 2010; Lu et al., 2018) and lacustrine sediments (Weber et al., 2015; Colcord et al., 2017; Lattaud et al., 2021). These studies list consistent arguments for a heterotrophic metabolism of brGDGT producers, including similar values and downcore correlation between $\delta^{13}C_{\rm TOC}$ and $\delta^{13}C$ values of brGDGT-derived alkanes and lack of inorganic carbon incorporation in stable isotope probing experiments.

Consistent with this reasoning, the δ^{13} C values of brGDGT-I and brGMGT-I reported here indicate a heterotrophic source organism for both compounds. Stratigraphic variations in the δ^{13} C profiles of brGDGT-I and brGMGT-I in the peat samples are related to shifts in $\delta^{13}C_{TOC}$ (Fig. 2), which we interpret to result from the utilization of a carbon source with an isotopic composition close to TOC. This is especially evident in core SEB1B, where minor $\delta^{13}C_{TOC}$ excursions at 38 and 48 cm are reflected in $\delta^{13}\text{C}$ values of brGDGT-I and brGMGT-I. In cores SEB2B and SEB2B-O, downcore trends in $\delta^{13}C_{TOC}$ are similarly reflected in $\delta^{13}C$ values of brGDGT-I and brGMGT-I. In the upper part (<20 cm sample depth) of core SEB2B, the δ^{13} C value of brGDGT-I is higher than $\delta^{13}C_{TOC}$, with an offset of up to 1.4 %. This pronounced enrichment contrasts with lower $\delta^{13}\text{C}$ values in the deeper part of the core, which suggests a similar influence of the ground water level as described above. Unfortunately, the lack of shallower samples in core SEB1B prevents a direct comparison and validation of trends between the two cores. Nevertheless, the 20 cm sample is the only sample where the δ^{13} C value of brGDGT-I is higher than $\delta^{13}C_{TOC}.$ Below this depth, $\delta^{13}C$ values decrease in both cores, so we will assume similar processes and effects in both cores.

Known brGDGT-producing Acidobacteria, such as Solibacter usitatus (Chen et al., 2022; Halamka et al., 2022), can use various carbon sources, including simple sugars, alcohols, and cellulose (Ward et al., 2009). A relative ¹³C-enrichment of brGDGT-derived alkanes and other bacterial biomarkers (i.e., hopanoids) has been attributed to the preferential utilization of 13C-enriched, labile substrates such as carbohydrates by the source organism (Huang et al., 1996; Pancost and Sinninghe Damsté, 2003; Weijers et al., 2006). Metagenomic analyses of the microbial community in a tropical peat swamp forest revealed (i) the overwhelming dominance of bacteria, with Acidobacteria and Proteobacteria as the two main groups, and (ii) the presence of versatile catabolic pathways for the degradation of lignocellulosic peat components (Kanokratana et al., 2011). Generally, availability of (hemi-)cellulose, carbohydrates, and protein decreases with depth in tropical peats due to microbial degradation (Yonebayashi et al., 1994). Specifically, Jackson et al. (2009) described highest aerobic cellulolytic microbial activity in the upper (i.e., < 10 cm) layers of a tropical Malaysian peat swamp forest, where Acidobacteria dominated the microbial community. This rapid decrease in extracellular enzyme activity may reflect a decrease in the availability of either oxygen or readily-degradable

organic substrates (Jackson et al., 2009). The distinctly higher brGDGT-I δ^{13} C values in the upper layers of the Sebangau peat may thus reflect preferential degradation of ¹³C-enriched organic matter (such as carbohydrates), possibly by Acidobacteria. In deeper peat layers, lower brGDGT-I δ^{13} C values suggest degradation of organic matter with δ^{13} C closer to TOC (such as proteins and nucleic acids), given that lipid biosynthesis generally produces molecular structures that are ¹³Cdepleted relative to biomass and TOC (Haves, 2001). Isotopic depletion of brGMGT-I relative to TOC of \sim 1–2 ‰ in most samples indicates carbon sources with δ^{13} C similar to that of TOC (proteins, nucleic acids) throughout all depth intervals. Consistent with these observations, depletion of brGMGT-I and brGDGT-I relative to TOC is also observed in the two Miocene lignite samples, but the low number of samples does not allow discerning depth trends in the lignites. Distinct carbon sources imply i) different source organisms of brGDGTs and brGMGTs and ii) production of these compounds over the entire peat profile.

It is probable that increased brGMGT abundances relative to brGDGTs at depths > 20 cm (Fig. 3a) reflect, or respond to, low oxygen availability/anoxia, given that this is also the depth of mean annual water levels at the study sites. It has generally been observed that oxygen concentration in soils and peats is controlled by water level and specifically that oxygen limitation may be an important driver of brGDGT and brGMGT production (e.g., Weijers et al., 2006; Peterse et al., 2011; Huguet et al., 2017; Naafs et al., 2018a; Halamka et al., 2021). At the oxic-anoxic transition zone (~20 cm depth), concentrations increase abruptly for brGMGTs and gradually for brGDGTs (Fig. S2). This distribution suggests that brGMGTs are produced predominantly under anaerobic conditions while brGDGTs are abundant over the entire oxygen concentration range, as suggested earlier (Naafs et al., 2018a). Higher brGMGT relative abundances under anaerobic conditions are likely not an artifact of higher preservation, as diagenetic stability of brGMGTs and brGDGTs is likely to be similar, with degradation initiating at the ether bonds (Liu et al., 2016). Instead, brGMGTs may preferentially, but not exclusively, be produced at low or no oxygen availability, consistent with the recent observation that oxygen limitation can trigger changes in brGDGT production in Acidobacteria (Halamka et al., 2021). We therefore interpret convergence of lipid δ^{13} C values at depth to be reflective of an in situ, microbial community producing both brGDGTs and brGMGTs using similar, micro-aerobic or anaerobic heterotrophic or fermentative metabolisms.

4.3. Sources of brGMGTs and their impacts on brGMGT proxies

The only known source of brGDGTs are Acidobacteria (e.g., Sinninghe Damsté et al., 2014; Halamka et al., 2021, 2022; Chen et al., 2022), which are abundant in peats and other environments where brGDGTs and brGMGTs have been found (Naafs et al., 2018a). Based on distinct branching patterns of the alkyl chains (13,16-dimethyl), brGDGTs can be distinguished from tetraether lipids produced by other bacteria (15,16-dimethyl; e.g., Lee et al., 1998; Sinninghe Damsté et al., 2007). These branching patterns have so far not been studied for brGMGTs (Liu et al., 2012; Naafs et al., 2018a). It is therefore possible that brGMGTs have a distinct branching pattern and are produced by bacteria other than Acidobacteria. However, the abundances of brGMGTs and their methylation and cyclization patterns are correlated to those of brGDGTs in a global compilation (Naafs et al., 2018a), suggesting common sources.

If brGDGTs and brGMGTs have identical sources, the offsets between their δ^{13} C values (more negative values in brGMGTs), could represent fractionation during biosynthesis of brGMGT from a brGDGT precursor. Although the pathways of brGDGT and brGMGT biosynthesis are not well constrained (Chen et al., 2022; Halamka et al., 2022), they could be broadly homologous to iGDGT biosynthesis (Lloyd et al., 2022; Zeng et al., 2022), and based on this analogy, carbon isotopic fractionation during biosynthesis is likely not of sufficient magnitude to explain the observed δ^{13} C offsets. During iGDGT biosynthesis, cyclopentyl ring

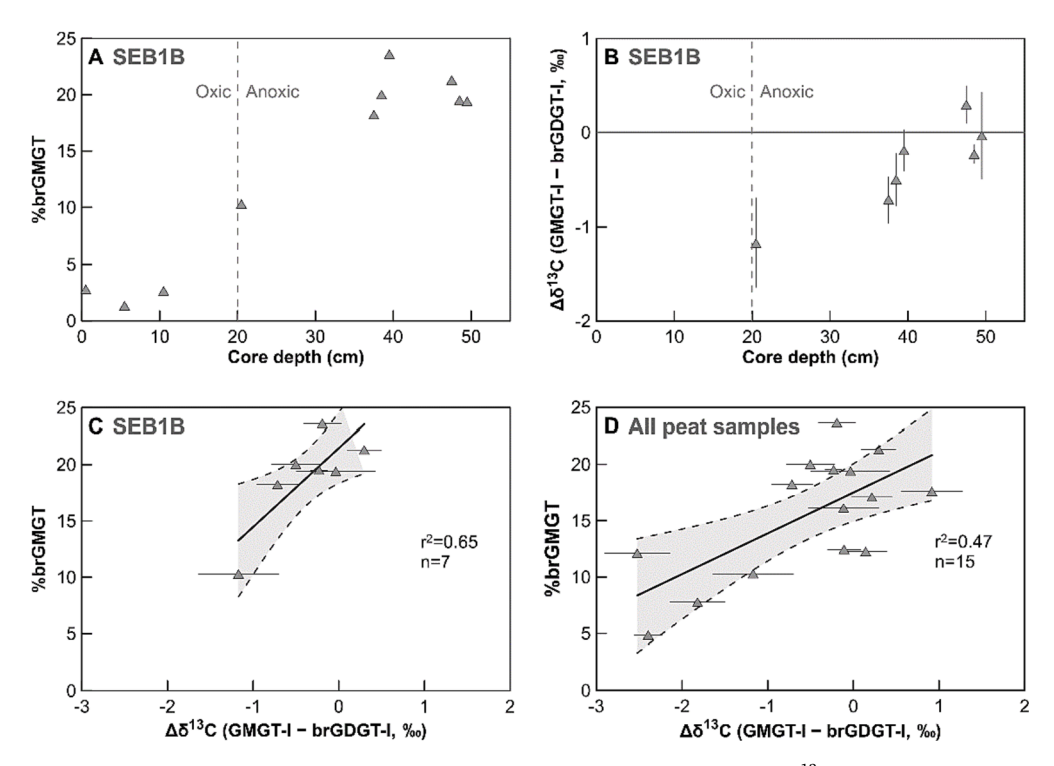


Fig. 3. Relative abundance of brGMGTs (%brGMGT, A) and carbon isotopic offsets of brGMGT-I and brGDGT-I ($\Delta\delta^{13}$ C brGMGT-I – brGDGT-I, B) showing core SEB1B as an example, and correlation (linear regression: solid black line; 95% confidence intervals: grey area and dashed lines) between offset and %brGMGT for SEB1B (C) and all peat samples (D). The tentative depth of the oxic-anoxic transition is indicated by a stippled vertical line in panels A and B.

moieties are formed through intramolecular carbon–carbon bonds without discernible carbon isotopic fractionation even after three consecutive steps of ring formation (Könneke et al., 2012). Therefore, we do not expect the single carbon–carbon bond formed during brGMGT biosynthesis to result in carbon isotopic fractionation of the magnitude required to explain the observed offset. Moreover, the offset between brGDGTs and brGMGTs is variable downcore (0 to $-2.5\,\%$) and between locations, which would not necessarily be expected if the offset were caused by biosynthesis.

Based on two lines of evidence, we suggest that brGDGTs and brGMGTs originate from overlapping but not identical sources. First, cultivated brGDGT-producing bacteria lack brGMGTs under the conditions tested to-date, including oxygen limitation (Sinninghe Damsté et al., 2014; Halamka et al., 2021, 2022; Chen et al., 2022), with the caveat that all identified brGDGT producers are (micro)aerobic. This indicates that at least some brGDGT producers do not (or are difficult to induce to) produce brGMGTs. Second, the abundance of brGMGTs relative to brGDGTs increases with depth in the Sebangau peat profiles. The relative abundance of brGMGTs previously has been shown to be positively correlated to temperature (Naafs et al., 2018a; Baxter et al., 2019), pointing to a role in membrane homeostasis analogous to the role of isoprenoid GMGTs in archaea (Schouten et al., 2008; Knappy et al., 2011; Sollich et al., 2017; Naafs et al., 2018a; Tourte et al., 2022). However, here the downcore trends are likely not recording past changes in temperature, as the studied Sebangau peats were deposited in tropical regions with little secular variation in regional air temperature during the last century (McAlpine et al., 2018).

The changes in relative abundance could be interpreted as a membrane adaptation to changes in physicochemical conditions (e.g., oxygen availability), and the concurrent carbon isotopic compositions of brGDGTs and brGMGTs point towards this adaptation being expressed by a transition between distinct source organisms. The δ^{13} C offset between brGDGTs and brGMGTs in the Sebangau peats is correlated to the relative abundance of brGMGTs (%brGMGT; Fig. 3). This offset becomes smaller at higher %brGMGT. This suggests (i) that at least some brGDGT

producers do not produce brGMGTs and (ii) that the brGMGT producers that also produce brGDGTs form a larger part of the total community at depth and possibly use a different carbon substrate compared to the shallower community. In the two Miocene lignite samples, the same relationship between $\delta^{13}\text{C}$ and %brGMGT is not observed (Fig. 2), which could be related to ongoing microbial activity after lignite formation (e. g., Gründger et al., 2015; Imachi et al., 2019) or the temperature effect on %brGMGTs (Naafs et al., 2018a). The lignites were deposited ~ 400 ka apart and under a generally warmer climate during the Miocene (Korasidis et al., 2019), which may have influenced %brGMGTs independent of community changes. Divergent sources of brGDGTs and brGMGTs in peats imply that in addition to a homeostatic response to temperature (e.g., Naafs et al., 2018a; Sluijs et al., 2020; Bijl et al., 2021), changes in bacterial community composition (driven by factors such as substrate availability, oxygenation, pH, and temperature) may influence proxies that are based on brGMGT relative abundance.

5. Conclusions

The carbon isotopic compositions of brGMGTs of brGDGTs in tropical peats and lignites are broadly similar to those of the TOC, which we interpret to reflect primarily heterotrophic metabolisms of the source organisms. Divergence in δ^{13} C of brGMGTs and brGDGTs, especially in the oxic part of the peat profiles, indicates that not all brGDGT producers make brGMGTs, consistent with the limited culture data available to date. We suggest that the relative abundance of brGMGTs may be dependent on community composition in addition to temperature, which could confound the use of brGMGT relative abundance in peat as a temperature proxy. However, it remains to be shown if this is also true for brGMGTs found in mineral soils as well as ocean and lake water columns and sediments, although we note that the slope of the regression between δ^{13} C and %brGMGT will be dependent on local climatic boundary conditions. The offsets in $\delta^{13}C$ between brGMGTs and brGDGTs point towards utilization of distinct carbon sources or distinct metabolic pathways, which could also be reflected in the fractionation of $% \left\{ 1\right\} =\left\{ 1\right\} =$ other isotopes, such as $^2\text{H}/^1\text{H}$ ratios. Therefore, studying the $^2\text{H}/^1\text{H}$ composition of brGMGTs and brGDGTs may help further discern their sources. Our work highlights the advantage of using SWiM-IRMS for enabling isotopic analysis of compound classes that are not amenable to conventional IRMS techniques. This method may also be applicable to the isotopic analysis of other "large" compounds such as C_{80} monoalkyl tetraacids commonly found in petroleum.

Data Availability

All data are available in the supplementary appendix and were deposited in the Pangaea repository (doi: 10.1594/PANGAEA.954301).

Declaration of Competing Interest

The authors declare that they have no known competing financial interests or personal relationships that could have appeared to influence the work reported in this paper.

Data availability

All data are available in the supplementary appendix and were deposited in the Pangaea repository

Acknowledgements

We thank Dr. Angela Gallego-Sala and Dr. Vera Korasidis for providing samples used in this work. We thank associate editor Rienk Smittenberg and two anonymous reviewers for constructive comments that helped improve an earlier version of this manuscript. Funding for this work was provided by the US National Science Foundation (1702262 and 1843285, to A.P.). L.K. was supported by Deutscher Akademischer Austauschdienst (DAAD RISE Worldwide Fellowship #US-ES-4055). F.J.E. was supported by the Deutsche Forschungsgemeinschaft (grant 441217575). B.D.A.N. acknowledges funding through a Royal Society Tata University Research Fellowship. V. L. was supported by funding from the Royal Society through the URF enhancement award of B.D.A.N.

Appendix A. Supplementary material

Supplementary data to this article can be found online at https://doi.org/10.1016/j.orggeochem.2023.104558.

References

- Balesdent, J., Girardin, C., Mariotti, A., 1993. Site-related 8¹³C of tree leaves and soil organic matter in a temperate forest. Ecology 74, 1713–1721.
- Baxter, A.J., Hopmans, E.C., Russell, J.M., Sinninghe Damsté, J.S., 2019. Bacterial GMGTs in East African lake sediments: Their potential as palaeotemperature indicators. Geochimica et Cosmochimica Acta 259, 155–169.
- Becker, K.W., Lipp, J.S., Zhu, C., Liu, X.-L., Hinrichs, K.-U., 2013. An improved method for the analysis of archaeal and bacterial ether core lipids. Organic Geochemistry 61, 34–44.
- Bijl, P.K., Frieling, J., Cramwinckel, M.J., Boschman, C., Sluijs, A., Peterse, F., 2021. Maastrichtian-Rupelian paleoclimates in the southwest Pacific – a critical reevaluation of biomarker paleothermometry and dinoflagellate cyst paleoecology at Ocean Drilling Program Site 1172. Climate of the Past 17, 2393–2425.
- Blewett, J., Elling, F.J., Naafs, B.D.A., Kattein, L., Evans, T.W., Lauretano, V., Gallego-Sala, A.V., Pancost, R.D., Pearson, A., 2022. Metabolic and ecological controls on the stable carbon isotopic composition of archaeal (isoGDGT and BDGT) and bacterial (brGDGT) lipids in wetlands and lignites. Geochimica et Cosmochimica Acta 320, 1–25.
- Brocks, J.J., Pearson, A., 2005. Building the biomarker tree of life. Reviews in Mineralogy and Geochemistry 59, 233–258.
- Chen, Y., Zheng, F., Yang, H., Yang, W., Wu, R., Liu, X., Liang, H., Chen, H., Pei, H., Zhang, C., Pancost, R.D., Zeng, Z., 2022. The production of diverse brGDGTs by an Acidobacterium providing a physiological basis for paleoclimate proxies. Geochimica et Cosmochimica Acta 337, 155–165.
- Clymo, R.S., 1984. The limits to peat bog growth. Philosophical Transactions of the Royal Society of London. B, Biological Sciences 303, 605–654.

- Colcord, D.E., Pearson, A., Brassell, S.C., 2017. Carbon isotopic composition of intact branched GDGT core lipids in Greenland lake sediments and soils. Organic Geochemistry 110, 25–32.
- Elling, F.J., Gottschalk, J., Doeana, K.D., Kusch, S., Hurley, S.J., Pearson, A., 2019. Archaeal lipid biomarker constraints on the Paleocene-Eocene carbon isotope excursion. Nature Communications 10, 4519.
- Esmeijer-Liu, A.J., Kürschner, W.M., Lotter, A.F., Verhoeven, J.T.A., Goslar, T., 2012. Stable carbon and nitrogen isotopes in a peat profile are influenced by early stage diagenesis and changes in atmospheric CO₂ and N deposition. Water, Air, & Soil Pollution 223, 2007–2022.
- Gründger, F., Jiménez, N., Thielemann, T., Straaten, N., Lüders, T., Richnow, H.-H., Krüger, M., 2015. Microbial methane formation in deep aquifers of a coal-bearing sedimentary basin, Germany. Frontiers in Microbiology 6.
- Halamka, T.A., McFarlin, J.M., Younkin, A.D., Depoy, J., Dildar, N., Kopf, S.H., 2021. Oxygen limitation can trigger the production of branched GDGTs in culture. Geochemical Perspectives Letters 19, 36–39.
- Halamka, T.A., Raberg, J.H., McFarlin, J.M., Younkin, A.D., Mulligan, C., Liu, X.-L., Kopf, S.H., 2022. Production of diverse brGDGTs by Acidobacterium Solibacter usitatus in response to temperature, pH, and O₂ provides a culturing perspective on brGDGT proxies and biosynthesis. Geobiology 21, 102–118.
- Hayes, J.M., 2001. Fractionation of carbon and hydrogen isotopes in biosynthetic processes. Reviews in Mineralogy and Geochemistry 43, 225–277.
- Huang, Y., Bol, R., Harkness, D.D., Ineson, P., Eglinton, G., 1996. Post-glacial variations in distributions, ¹³C and ¹⁴C contents of aliphatic hydrocarbons and bulk organic matter in three types of British acid upland soils. Organic Geochemistry 24, 273-287
- Huguet, A., Meador, T.B., Laggoun-Défarge, F., Könneke, M., Wu, W., Derenne, S., Hinrichs, K.-U., 2017. Production rates of bacterial tetraether lipids and fatty acids in peatland under varying oxygen concentrations. Geochimica et Cosmochimica Acta 203, 103–116.
- Imachi, H., Tasumi, E., Takaki, Y., Hoshino, T., Schubotz, F., Gan, S., Tu, T.-H., Saito, Y., Yamanaka, Y., Ijiri, A., Matsui, Y., Miyazaki, M., Morono, Y., Takai, K., Hinrichs, K.-U., Inagaki, F., 2019. Cultivable microbial community in 2-km-deep, 20-million-year-old subseafloor coalbeds through ~1000 days anaerobic bioreactor cultivation. Scientific Reports 9, 2305.
- Itoh, M., Okimoto, Y., Hirano, T., Kusin, K., 2017. Factors affecting oxidative peat decomposition due to land use in tropical peat swamp forests in Indonesia. Science of The Total Environment 609, 906–915.
- Jackson, C.R., Liew, K.C., Yule, C.M., 2009. Structural and functional changes with depth in microbial communities in a tropical malaysian peat swamp forest. Microbial Ecology 57, 402–412.
- Kanokratana, P., Uengwetwanit, T., Rattanachomsri, U., Bunterngsook, B., Nimchua, T., Tangphatsornruang, S., Plengvidhya, V., Champreda, V., Eurwilaichitr, L., 2011. Insights into the phylogeny and metabolic potential of a primary tropical peat swamp forest microbial community by metagenomic analysis. Microbial Ecology 61, 518–528.
- Kirkels, F.M.S.A., Usman, M.O., Peterse, F., 2022. Distinct sources of bacterial branched GMGTs in the Godavari River basin (India) and Bay of Bengal sediments. Organic Geochemistry 167, 104405.
- Knappy, C., Barillà, D., Chong, J., Hodgson, D., Morgan, H., Suleman, M., Tan, C., Yao, P., Keely, B., 2015. Mono-, di- and trimethylated homologues of isoprenoid tetraether lipid cores in archaea and environmental samples: Mass spectrometric identification and significance. Journal of Mass Spectrometry 50, 1420–1432.
- Knappy, C.S., Nunn, C.E.M., Morgan, H.W., Keely, B.J., 2011. The major lipid cores of the archaeon *Ignisphaera aggregans*: implications for the phylogeny and biosynthesis of glycerol monoalkyl glycerol tetraether isoprenoid lipids. Extremophiles 15, 517–528.
- Könneke, M., Lipp, J.S., Hinrichs, K.-U., 2012. Carbon isotope fractionation by the marine ammonia-oxidizing archaeon *Nitrosopumilus maritimus*. Organic Geochemistry 48, 21–24.
- Korasidis, V.A., Wallace, M.W., Wagstaff, B.E., Hill, R.S., 2019. Terrestrial cooling record through the Eocene-Oligocene transition of Australia. Global and Planetary Change 173, 61–72.
- Langworthy, T.A., 1977. Long-chain diglycerol tetraethers from *Thermoplasma acidophilum*. Biochimica et Biophysica Acta (BBA) Lipids and Lipid. Metabolism 487, 37–50.
- Lattaud, J., De Jonge, C., Pearson, A., Elling, F.J., Eglinton, T.I., 2021. Microbial lipid signatures in Arctic deltaic sediments – Insights into methane cycling and climate variability. Organic Geochemistry 157, 104242.
- Lee, J., Jung, S., Lowe, S., Zeikus, J.G., Hollingsworth, R.I., 1998. A dynamically regulated transformation of a bacterial bilayer membrane to a cross-linked 2dimensional sheet during adaptation to unfavorable environmental pressures. Journal of the American Chemical Society 120, 5855–5863.
- Liu, X.L., Summons, R.E., Hinrichs, K.U., 2012. Extending the known range of glycerol ether lipids in the environment: Structural assignments based on tandem mass spectral fragmentation patterns. Rapid Communications in Mass Spectrometry 26, 2295–2302.
- Liu, X.L., Birgel, D., Elling, F.J., Sutton, P.A., Lipp, J.S., Zhu, R., Zhang, C., Könneke, M., Peckmann, J., Rowland, S.J., Summons, R.E., Hinrichs, K.U., 2016. From ether to acid: A plausible degradation pathway of glycerol dialkyl glycerol tetraethers. Geochimica et Cosmochimica Acta 183, 138–152.
- Lloyd, C.T., Iwig, D.F., Wang, B., Cossu, M., Metcalf, W.W., Boal, A.K., Booker, S.J., 2022. Discovery, structure, and mechanism of a tetraether lipid synthase. Nature 609, 197–203.

- Lu, H., Liu, W., Sheng, W., 2018. Carbon isotopic composition of branched tetraether membrane lipids in a loess-paleosol sequence and its geochemical significance. Palaeogeography, Palaeoclimatology, Palaeoecology 504, 150–155.
- Lü, X., Liu, X., Xu, C., Song, J., Li, X., Yuan, H., Li, N., Wang, D., Yuan, H., Ye, S., 2019. The origins and implications of glycerol ether lipids in China coastal wetland sediments. Scientific Reports 9, 18529.
- McAlpine, C.A., Johnson, A., Salazar, A., Syktus, J., Wilson, K., Meijaard, E., Seabrook, L., Dargusch, P., Nordin, H., Sheil, D., 2018. Forest loss and Borneo's climate. Environmental Research Letters 13, 044009.
- Morii, H., Eguchi, T., Nishihara, M., Kakinuma, K., Konig, H., Koga, Y., 1998. A novel ether core lipid with H-shaped C₈₀-isoprenoid hydrocarbon chain from the hyperthermophilic methanogen *Methanothermus fervidus*. Biochimica et Biophysica Acta 1390, 339–345.
- Naafs, B.D.A., Inglis, G.N., Zheng, Y., Amesbury, M.J., Biester, H., Bindler, R., Blewett, J., Burrows, M.A., del Castillo Torres, D., Chambers, F.M., Cohen, A.D., Evershed, R.P., Feakins, S.J., Gałka, M., Gallego-Sala, A., Gandois, L., Gray, D.M., Hatcher, P.G., Honorio Coronado, E.N., Hughes, P.D.M., Huguet, A., Könönen, M., Laggoun-Défarge, F., Lähteenoja, O., Lamentowicz, M., Marchant, R., McClymont, E., Pontevedra-Pombal, X., Ponton, C., Pourmand, A., Rizzuti, A.M., Rochefort, L., Schellekens, J., De Vleeschouwer, F., Pancost, R.D., 2017. Introducing global peat-specific temperature and pH calibrations based on brGDGT bacterial lipids. Geochimica et Cosmochimica Acta 208, 285–301.
- Naafs, B.D.A., McCormick, D., Inglis, G.N., Pancost, R.D., 2018a. Archaeal and bacterial H-GDGTs are abundant in peat and their relative abundance is positively correlated with temperature. Geochimica et Cosmochimica Acta 227, 156–170.
- Naafs, B.D.A., Rohrssen, M., Inglis, G.N., Lähteenoja, O., Feakins, S.J., Collinson, M.E., Kennedy, E.M., Singh, P.K., Singh, M.P., Lunt, D.J., Pancost, R.D., 2018b. High temperatures in the terrestrial mid-latitudes during the early Palaeogene. Nature Geoscience 11, 766–771.
- Naafs, B.D.A., Inglis, G.N., Blewett, J., McClymont, E.L., Lauretano, V., Xie, S., Evershed, R.P., Pancost, R.D., 2019. The potential of biomarker proxies to trace climate, vegetation, and biogeochemical processes in peat: A review. Global and Planetary Change 179, 57–79.
- Natelhoffer, K.J., Fry, B., 1988. Controls on natural nitrogen-15 and carbon-13 abundances in forest soil organic matter. Soil Science Society of America Journal 52, 1633–1640.
- Novák, M., Buzek, F., Adamová, M., 1999. Vertical trends in δ^{13} C, δ^{15} N and δ^{34} S ratios in bulk Sphagnum peat. Soil Biology and Biochemistry 31, 1343–1346.
- Pancost, R.D., Sinninghe Damsté, J.S., 2003. Carbon isotopic compositions of prokaryotic lipids as tracers of carbon cycling in diverse settings. Chemical Geology 195, 29–58.
- Pearson, A., Hurley, S.J., Walter, S.R.S., Kusch, S., Lichtin, S., Zhang, Y.G., 2016. Stable carbon isotope ratios of intact GDGTs indicate heterogeneous sources to marine sediments. Geochimica et Cosmochimica Acta 181, 18–35.
- Pearson, A., Ingalls, A.E., 2013. Assessing the use of archaeal lipids as marine environmental proxies. Annual Review of Earth and Planetary Sciences 41, 359–384. Peterse, F., Hopmans, E.C., Schouten, S., Mets, A., Rijpstra, W.I.C., Sinninghe Damsté, J.
- Peterse, F., Hopmans, E.C., Schouten, S., Mets, A., Rijpstra, W.I.C., Sinninghe Damsté, J. S., 2011. Identification and distribution of intact polar branched tetraether lipids in peat and soil. Organic Geochemistry 42. 1007–1015.
- Polik, C.A., Elling, F.J., Pearson, A., 2018. Impacts of paleoecology on the TEX₈₆ sea surface temperature proxy in the Pliocene-Pleistocene Mediterranean Sea. Paleoceanography and Paleoclimatology 33, 1472–1489.
- Rosa, M.D., Gambacorta, A., Gliozzi, A., 1986. Structure, biosynthesis, and physicochemical properties of archaebacterial lipids. Microbiological Reviews 50, 70–80
- Schouten, S., Hopmans, E.C., Pancost, R.D., Sinninghe Damsté, J.S., 2000. Widespread occurrence of structurally diverse tetraether membrane lipids: Evidence for the ubiquitous presence of low-temperature relatives of hyperthermophiles. Proceedings of the National Academy of Sciences 97, 14421–14426.
- Schouten, S., Baas, M., Hopmans, E.C., Sinninghe Damsté, J.S., 2008. An unusual isoprenoid tetraether lipid in marine and lacustrine sediments. Organic Geochemistry 39, 1033–1038.
- Schouten, S., Hopmans, E.C., Sinninghe Damsté, J.S., 2013. The organic geochemistry of glycerol dialkyl glycerol tetraether lipids: A review. Organic Geochemistry 54, 19–61.
- Sessions, A.L., Sylva, S.P., Hayes, J.M., 2005. Moving-wire device for carbon isotopic analyses of nanogram quantities of nonvolatile organic carbon. Analytical Chemistry 77, 6519–6527.
- Sinninghe Damsté, J.S., Hopmans, E.C., Pancost, R.D., Schouten, S., Geenevasen, J.A.J., 2000. Newly discovered non-isoprenoid glycerol dialkyl glycerol tetraether lipids in sediments. Chemical Communications 1683–1684.
- Sinninghe Damsté, J.S., Rijpstra, W.I.C., Hopmans, E.C., Schouten, S., Balk, M., Stams, A. J.M., 2007. Structural characterization of diabolic acid-based tetraester, tetraether and mixed ether/ester, membrane-spanning lipids of bacteria from the order *Thermotogales*. Archives of Microbiology 188, 629–641.
- Sinninghe Damsté, J.S., Rijpstra, W.I.C., Hopmans, E.C., Foesel, B.U., Wüst, P.K., Overmann, J., Tank, M., Bryant, D.A., Dunfield, P.F., Houghton, K., Stott, M.B., 2014. Ether- and ester-bound *iso* -diabolic acid and other lipids in members of

- Acidobacteria subdivision 4. Applied and Environmental Microbiology 80, 5207–5218
- Sluijs, A., Frieling, J., Inglis, G.N., Nierop, K.G.J., Peterse, F., Sangiorgi, F., Schouten, S., 2020. Late Paleocene-early Eocene Arctic Ocean sea surface temperatures: reassessing biomarker paleothermometry at Lomonosov Ridge. Climate of the Past 16, 2381–2400.
- Smith, B.N., 1972. Natural abundance of the stable isotopes of carbon in biological systems. Bioscience 22, 226–231.
- Sollich, M., Yoshinaga, M.Y., Häusler, S., Price, R.E., Hinrichs, K.-U., Bühring, S.I., 2017. Heat stress dictates microbial lipid composition along a thermal gradient in marine sediments. Frontiers in Microbiology 8, 1550.
- Stout, J.D., Goh, K.M., Rafter, T.A., 1981. Chemistry and turnover of naturally occurring resistant organic compounds in soil. In: Paul, E.A., Ladd, J.N. (Eds.), Soil Biochemistry. CRC Press, Boca Raton, pp. 1–74.
- Sugai, A., Uda, I., Itoh, Y.H., Itoh, T., 2004. The core lipid composition of the 17 strains of hyperthermophilic Archaea, *Thermococcales*. Journal of Oleo Science 53, 41–44.
- Tang, X., Naafs, B.D.A., Pancost, R.D., Liu, Z., Fan, T., Zheng, Y., 2021. Exploring the influences of temperature on "H-Shaped" glycerol dialkyl glycerol tetraethers in a stratigraphic context: Evidence from two peat cores across the Late Quaternary. Frontiers in Earth Science 8, 541685.
- Tourte, M., Schaeffer, P., Grossi, V., Oger, P.M., 2022. Membrane adaptation in the hyperthermophilic archaeon Pyrococcus furiosus relies upon a novel strategy involving glycerol monoalkyl glycerol tetraether lipids. Environmental Microbiology 24, 2029–2046.
- Ward, N.L., Challacombe, J.F., Janssen, P.H., Henrissat, B., Coutinho, P.M., Wu, M., Xie, G., Haft, D.H., Sait, M., Badger, J., Barabote, R.D., Bradley, B., Brettin, T.S., Brinkac, L.M., Bruce, D., Creasy, T., Daugherty, S.C., Davidsen, T.M., DeBoy, R.T., Detter, J.C., Dodson, R.J., Durkin, A.S., Ganapathy, A., Gwinn-Giglio, M., Han, C.S., Khouri, H., Kiss, H., Kothari, S.P., Madupu, R., Nelson, K.E., Nelson, W.C., Paulsen, I., Penn, K., Ren, Q., Rosovitz, M.J., Selengut, J.D., Shrivastava, S., Sullivan, S.A., Tapia, R., Thompson, L.S., Watkins, K.L., Yang, Q., Yu, C., Zafar, N., Zhou, L., Kuske, C.R., 2009. Three genomes from the phylum *Acidobacteria* provide insight into the lifestyles of these microorganisms in soils. Applied and Environmental Microbiology 75, 2046–2056.
- Weber, Y., De Jonge, C., Rijpstra, W.I.C., Hopmans, E.C., Stadnitskaia, A., Schubert, C.J., Lehmann, M.F., Sinninghe Damsté, J.S., Niemann, H., 2015. Identification and carbon isotope composition of a novel branched GDGT isomer in lake sediments: Evidence for lacustrine branched GDGT production. Geochimica et Cosmochimica Acta 154, 118–129.
- Weijers, J.W.H., Schouten, S., Hopmans, E.C., Geenevasen, J.A.J., David, O.R.P., Coleman, J.M., Pancost, R.D., Sinninghe Damsté, J.S., 2006. Membrane lipids of mesophilic anaerobic bacteria thriving in peats have typical archaeal traits. Environmental Microbiology 8, 648–657.
- Weijers, J.W.H., Panoto, E., van Bleijswijk, J., Schouten, S., Rijpstra, W.I.C., Balk, M., Stams, A.J.M., Damsté, J.S.S., 2009. Constraints on the biological source(s) of the orphan branched tetraether membrane lipids. Geomicrobiology Journal 26, 402–414
- Weijers, J.W.H., Wiesenberg, G.L.B., Bol, R., Hopmans, E.C., Pancost, R.D., 2010. Carbon isotopic composition of branched tetraether membrane lipids in soils suggest a rapid turnover and a heterotrophic life style of their source organism(s). Biogeosciences 7, 2959–2973
- Weiss, D., Shotyk, W., Rieley, J., Page, S., Gloor, M., Reese, S., Martinez-Cortizas, A., 2002. The geochemistry of major and selected trace elements in a forested peat bog, Kalimantan, SE Asia, and its implications for past atmospheric dust deposition. Geochimica et Cosmochimica Acta 66, 2307–2323.
- Wu, M.S., West, A.J., Feakins, S.J., 2019. Tropical soil profiles reveal the fate of plant wax biomarkers during soil storage. Organic Geochemistry 128, 1–15.
- Wüst, R.A.J., Jacobsen, G.E., von der Gaast, H., Smith, A.M., 2008. Comparison of radiocarbon ages from different organic fractions in tropical peat cores: insights from Kalimantan, Indonesia. Radiocarbon 50, 359–372.
- Xie, S., Liu, X.L., Schubotz, F., Wakeham, S.G., Hinrichs, K.U., 2014. Distribution of glycerol ether lipids in the oxygen minimum zone of the Eastern Tropical North Pacific Ocean. Organic Geochemistry 71, 60–71.
- Yonebayashi, K., Pechayapisit, J., Vijarnsorn, P., Zahari, A.B., Kyuma, K., 1994. Chemical alterations of tropical peat soils determined by Waksman's proximate analysis and properties of humic acids. Soil Science and Plant Nutrition 40, 435–444.
- Zeng, Z., Chen, H., Yang, H., Chen, Y., Yang, W., Feng, X., Pei, H., Welander, P.V., 2022. Identification of a protein responsible for the synthesis of archaeal membrane-spanning GDGT lipids. Nature Communications 13, 1545.
- Zhu, C., Lipp, J.S., Wörmer, L., Becker, K.W., Schröder, J., Hinrichs, K.U., 2013. Comprehensive glycerol ether lipid fingerprints through a novel reversed phase liquid chromatography-mass spectrometry protocol. Organic Geochemistry 65, 53-62.
- Zhu, C., Yoshinaga, M.Y., Peters, C.A., Liu, X.L., Elvert, M., Hinrichs, K.U., 2014. Identification and significance of unsaturated archaeal tetraether lipids in marine sediments. Rapid Communications in Mass Spectrometry 28, 1144–1152.